

THREE-DIMENSIONAL GUSTS FOR THE PREDICTION OF TONAL FAN NOISE

J. de Laborderie and S. Moreau

Groupe d'Acoustique de l'Université de Sherbrooke (GAUS),
Mechanical Engineering Department, University of Sherbrooke,
SHERBROOKE, Qc, J1K2R1, CANADA
jerome.de.laborderie@usherbrooke.ca, stephane.moreau@usherbrooke.ca

ABSTRACT

In the framework of improving the tonal fan noise prediction the present study aims at evaluating the effects of 3D gusts in a cascade based acoustic model. Indeed they allow a better description of the excitation than the usual 2D decomposition. The 3D model accounting for the duct geometry is applied to an axial compressor stage for the tonal noise created by the rotor-stator interaction. An unsteady compressible flow simulation of this compressor provides both the excitation and the actual acoustic sources on the stator vane. Comparisons with the 2D version of the model and the results of the simulation are performed on the cascade response and on the acoustic power radiated within the duct. They show the improvements brought by the 3D model as well as some limitations that are analyzed.

NOMENCLATURE

B	Number of rotor blades	k_r	Radial wavenumber
C	Chord length	m	Order of azimuthal duct mode
M_c	Chordwise Mach number	q	Index of harmonics frequency
M_x	Axial Mach number	r, θ, x	Cylindrical coordinates
T_r	Radial period	s	Pitch
V	Number of stator vanes	H	Relative to hub
a	Index of passage mode	τ	Relative to tip
c_0	Speed of sound	χ_s	Vane stagger angle
d	Chordwise non-overlapped length	$\Gamma_{m,\mu}$	Normalisation function
h	Normal blade-to-blade length	μ	Order of radial duct mode
k	Index of cascade mode	Ω	Rotational speed

INTRODUCTION

The noise emitted by the fan stage of a modern turbofan aero-engine significantly contributes to the overall engine noise, especially at approach conditions. Among the fan noise acoustic sources, the interaction of the mean rotor wakes with the downstream stator vanes corresponds to the main contribution to the tonal noise. Several analytical models have been developed addressing this specific problem as they are more affordable

than Computational Aero-Acoustics (CAA) approaches for parametric studies. Among the acoustic models based on a cascade response, a first category considering a rectilinear cascade to radiate the noise and including the effects of 3D gusts has been widely studied for tonal and broadband noise (e.g. Glegg (1999), Hanson (2001) and Lloyd and Peake (2008)). The spanwise variation of the geometry might be introduced by splitting the vanes into strips and directly summing the acoustic powers of each strip. The second category also resorts to a strip theory but allows to radiate the acoustic field on the real duct modes. Meyer and Envia (1996) dealt with a 2D cascade response, and more recently Posson et al. (2011) considered a real 3D vortical disturbance interacting with the cascade. Whereas this model has only been applied to broadband noise studies, the current work focuses on the effect of introducing 3D gusts in the prediction of tonal fan noise.

The objective of the present study consists in evaluating this 3D analytical model on a realistic test case, i.e. a low pressure axial compressor stage. An unsteady flow simulation of this compressor has been performed and validated in Soulat et al. (2011) allowing on the one hand to extract the real excitation for the acoustic model and on the other hand to record the actual acoustic sources located on the vane surface. After a description of the 3D model with the methodology for considering skewed gusts, the following section presents the flow simulation. Finally the results of the 3D model are shown and analyzed in the last two sections and compared to the 2D version of the model and to the Computational Fluid Dynamics (CFD) response considered here as the reference.

CASCADE BASED ACOUSTIC MODEL

Analytical cascade response function

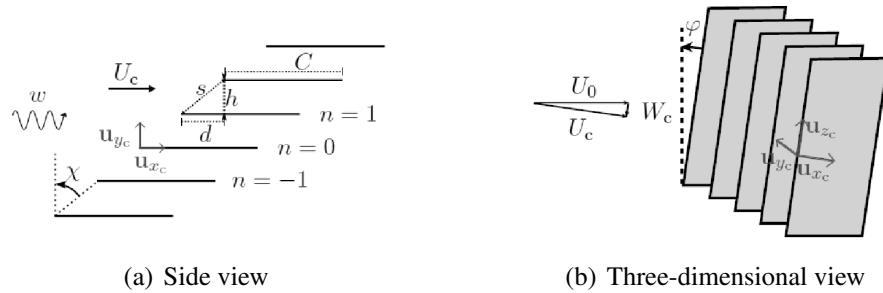


Figure 1: Geometry of the rectilinear cascade.

Posson et al. (2011) recently presented an acoustic model for the broadband noise due to rotor-stator interaction. It could also be relevant for tonal noise for which the excitation impinging on the stator vanes corresponds to the velocity deficit of the rotor wake. Following the strip theory, both the incident perturbation and the vane row are split into annular strips along the span and unwrapped. Each strip is modeled as a frozen perturbation interacting with a rectilinear cascade of perfectly thin and rigid flat plates of infinite span and finite chord C as shown in Fig. 1. The vanes can be staggered at an angle χ_s and swept at an angle φ . The mean flow U_0 is assumed parallel to the vane surface with zero incidence angle. The incident excitation is expanded as a sum of harmonic gusts with a Fourier transform. The unsteady vane loading produced by the cascade-gust interaction is predicted analytically (Posson et al., 2010) from an extension of the cascade model of Glegg (1999). The present unsteady vane loading formulation accounting for a

3D incident gust impinging on a 3D rectilinear cascade has been validated in a rectilinear configuration by comparing with alternative models (Posson et al., 2010). The unsteady vane loadings are seen as a distribution of equivalent acoustic dipoles which radiate in the annular duct as explained at the end of this section.

3D excitation

For the tonal noise created by the rotor-stator interaction, the previous cascade response function has only been used in its 2D form in de Laborderie et al. (2012). Since the excitation impinging on the cascade, corresponding to the normal upwash velocity on the vane $w = \vec{V} \cdot \vec{n}$, is $2\pi/B$ -periodic in the azimuthal direction, it can be split into a Fourier series with the coefficients W_q . Only the q^{th} coefficient of the excitation contributes to the cascade response at the q^{th} harmonic of the Blade Passing Frequency (BPF). Each gust of this excitation is characterized by its frequency $qB\Omega$ and its inter-blade phase angle $\sigma = 2\pi qB/V$. Since the absolute flow velocity is zero both at the hub and at the tip in a ducted turbomachine, the upwash velocity can also be Fourier transformed in the radial direction with a period $T_r = R_T - R_H$ to give the double Fourier series:

$$w(r, \theta, x) = \sum_{q=-\infty}^{+\infty} \sum_{n=-\infty}^{+\infty} W_{q,n}(x) e^{-iqB\theta} e^{-ik_r r} \text{ with } W_{q,n}(x) = \frac{1}{T_r} \int_{R_H}^{R_T} W_q(r, x) e^{+ik_r r} dr \quad (1)$$

where $k_r = 2\pi n/T_r$, $n \in \mathbb{Z}$, is the spanwise wavenumber.

Acoustic propagation

At each radius r the cascade response function of Posson et al. (2011) provides the pressure jump in the frequency domain across the stator vane $\Delta\hat{P}_0(x', r)$ for each gust $(qB\Omega, \sigma, k_r)$, where x' is the chordwise coordinate along the flat plate. Then for each q^{th} harmonic of the BPF, the acoustic source is written as:

$$\Delta\hat{P}_q(x', r) = \sum_{n=-\infty}^{+\infty} W_{q,n} \Delta\hat{P}_0(x', r) e^{-ik_r r}. \quad (2)$$

The unsteady vane loadings in Eq. (2) are used as dipole sources in an acoustic analogy. Assuming that the stator is placed in an infinite annular duct containing a uniform axial mean flow ($U_x = c_0 M_x$) (neither rotor nor mean swirl effects on the upstream propagation), Goldstein (1976) gives the formulation of the modal acoustic coefficient using the Green's function tailored to this configuration (see de Laborderie et al. (2012)), the superscripts $+$ and $-$ being for the upstream and downstream propagations respectively :

$$P_{q,m,\mu}^{\pm} = \frac{V}{2\Gamma_{m,\mu} \kappa_{m,\mu}} \int_{R_H}^{R_T} E_{m,\mu}(r) \left(\frac{m}{r} \cos \chi_s - k_{m,\mu}^{\pm} \sin \chi_s \right) L_{q,m,\mu} dr, \quad (3)$$

with:

$$k_{m,\mu}^{\pm} = \frac{M_x q B \Omega / c_0 \pm \kappa_{m,\mu}}{1 - M_x^2}, \quad \kappa_{m,\mu}^2 = \left(\frac{q B \Omega}{c_0} \right)^2 - \beta^2 \chi_{m,\mu}^2, \quad \beta^2 = 1 - M_x^2,$$

$$L_{q,m,\mu} = \int_0^C \Delta \hat{P}_q(x', r) e^{ik_{m,\mu}^{\pm} x'} dx' \quad \text{and} \quad k_{m,\mu}^{\pm} = k_{m,\mu}^{\pm} \cos \chi_s - \frac{m}{r} \sin \chi_s.$$

$k_{m,\mu}^{\pm}$ is the acoustic wavenumber in the duct axis direction. $E_{m,\mu}$ is the duct radial function and $\chi_{m,\mu}$ the duct eigenvalue. Finally the acoustic power of the q^{th} harmonic of the BPF reads after integration on a duct section (Meyer and Envia, 1996):

$$\Pi_q^{\pm} = \frac{\Gamma_{m,\mu}}{\rho_0 c_0^2} \sum_{m=-\infty}^{+\infty} \sum_{\mu=0}^{+\infty} \frac{\beta^4 q B \Omega \kappa_{m,\mu}}{(q B \Omega / c_0 \pm M_x \kappa_{m,\mu})^2} |P_{q,m,\mu}^{\pm}|^2. \quad (4)$$

The power of Eq. (4) is the sum over the contributions of the azimuthal and radial acoustic duct modes of indices m and μ respectively. This sum is limited to the cut-on modes for which $\kappa_{m,\mu}^2 > 0$. Moreover only the duct modes excited by the rotor-stator interaction are considered. They are given by the rule of Tyler and Sofrin (1962): $m = qB \pm zV, z \in \mathbb{N}$.

CME2 COMPRESSOR SIMULATION

Geometry and flow simulation parameters

The test case chosen for the present aeroacoustic study is the CME2 research compressor currently located and tested at the Laboratoire de Mecanique de Lille (LML) in France. It is a subsonic low-pressure single stage axial compressor with a 30 blade rotor upstream of a 40 vane stator, which are mounted in an annular duct with a hub-to-tip ratio of $R_H/R_T = 0.77$. The solidity at midspan of the stator is around 2 therefore cascade effects on the acoustic sources are expected to be significant. The rotational speed is 6300 RPM at nominal conditions, giving a blade passing frequency of BPF = 3150 Hz. At this operating point the flow rate is $11 \text{ kg}\cdot\text{s}^{-1}$ and the total pressure ratio of the stage is 1.14.

Recently Soulat et al. (2011) performed a full 3D unsteady compressible flow simulation of the CME2 compressor stage. The Navier-Stokes solver TurbFlow, developed at Ecole Centrale de Lyon, France, was chosen for this simulation as it is specifically designed for turbomachinery applications. This solver is based on a finite volume formulation and solves the conservative equations on a multiblock structured grid. The CME2 mesh is composed of about 3.9 million grid points distributed in 47 blocks. The mesh is refined close to the blades and casing walls to reach dimensionless cell sizes at the wall mostly comprised between $y^+ = 1$ to 5, corresponding to the level required for an accurate turbulence simulation with the Kok's $k - \omega$ turbulence model. The duct is divided by the rotor-stator interface, a plane axially located at 8% of chord upstream of the vane leading edge. The contact between rotating and fixed blocks is achieved using a slip contact condition. The flow-field is transferred through this contact using a high-order Fourier decomposition and recomposition with adequate angular phase in the azimuthal direction. The computational domain is composed of 3 rotor blades and 4 stator vanes so that chorochronic computations are not required. Indeed the interaction forces modes the orders of which are multiples of 10; the computational domain always contains an integer number of full azimuthal periods. The conservative flow variables are spatially discretized using the second-order Jameson centered scheme. Moreover the average cell

size in the blade and vane passages as well as in the row spacing is such that the aerodynamic wavelength corresponding to the third harmonic of the excitation (3 BPF) is spatially discretized by almost 20 grid points. With a second-order scheme, this ensures low dissipation and dispersion in the convection of the excitation harmonics up to 3 BPF.

Flow field and extraction of the unsteady vane loading

The compressor flow simulation has been validated by Soulat et al. (2011) against numerical and experimental data. As an illustration of the flow topology, Fig. 2 presents an instantaneous axial Mach number field at midspan. The boundary layers on both sides of the rotor blades form the wakes downstream of the blade trailing edges and are then convected with the mean flow. They interact with the stator vanes and are still visible downstream of the stator. Using the real unsteady simulation the pressure fluctuations on each gridpoint of a vane surface are extracted in time. It has been checked in Blandeau et al. (2012) that a convergence in the frequency domain is reached with a recording time of 12 blade passing periods. These timeseries of pressure are then Fourier transformed to obtain the pressure jumps $\Delta\hat{P}_q(x', r)$ of Eq. (2) and are considered here as the reference for the acoustic model. These realistic acoustic sources are finally propagated within the duct using the acoustic analogy described in the previous section, assuming that they are distributed on an equivalent flat plate staggered along the tangent to the mean camber line at the leading edge of the vane. The cascade of the model also uses this stagger angle following the recommendation of a previous study in Blandeau et al. (2012).

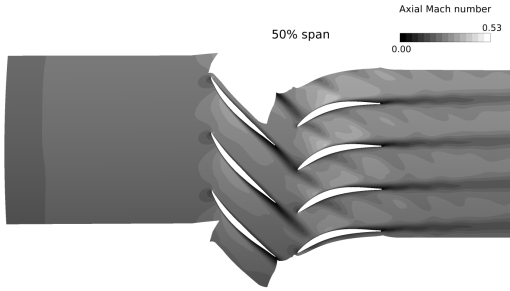


Figure 2: Instantaneous blade-to-blade axial Mach number field at midspan.

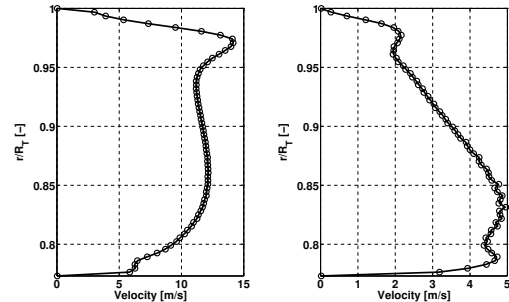


Figure 3: Azimuthal Fourier coefficients $W_q(r)$ of the upwash velocity, for $q = 1, 3$. Line: original coefficients, circles: reconstructed coefficients.

Decomposition of the excitation

The upwash velocity w impinging on the stator vanes corresponds to the vortical excitation for the acoustic model. It is extracted at the rotor-stator interface plane and time-averaged in the rotor reference frame over the three rotor blade passages. This allows a spatial averaging of the potential effects of the stator vanes. This excitation is regularly discretized in the azimuthal and radial directions and finally decomposed using Eq. (1). In order to verify that the present radial decomposition is relevant, the original azimuthal Fourier coefficients W_q are compared to their reconstruction in Fig. 3. Even if the sum is

infinite in Eq. (1) it is here limited to the interval $[-n_{max}, +n_{max}]$ with n_{max} corresponding to half the number of discretization points in the radial period. It is shown that for each of the considered harmonics the reconstructed signal perfectly matches the original Fourier coefficient over the whole span. Thus the method presented above and using the span as the radial period of the excitation is validated.

RESULTS - CASCADE RESPONSE

Limitation over the radial wavenumbers

In the cascade response (Eq. (2)) the sum over the radial wavenumbers is theoretically infinite and practically limited to the interval $[-n_{max}, +n_{max}]$. However it can be verified that the vane response is negligible for high values of $|k_r|$ whereas their computation is time-consuming. Thus a relevant criterion has to be found to only consider the gusts significantly contributing to the response. As explained in the second section the basic mechanism of the model corresponds to a gust $(qB\Omega, \sigma, k_r)$ convected with the chordwise Mach number M_c and impinging on a rectilinear cascade of infinite span. This cascade radiates acoustic modes of indices k among which some are cut-on and the others are cut-off. This behavior depends on their cut-off frequency $f_{c,k}$ (Posson et al. (2011)):

$$f_{c,k} = \frac{c_0}{2\pi s^2} \left[M_c d (\sigma - 2\pi k) \pm \sqrt{d^2 + \beta^2 h^2 \sqrt{(\sigma - 2\pi k)^2 + k_r^2 s^2}} \right]. \quad (5)$$

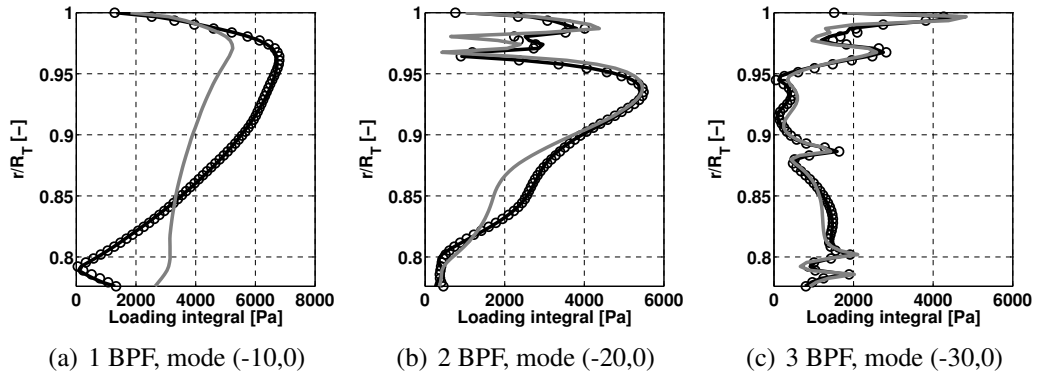


Figure 4: Amplitude of the cascade response (integrand of Eq. (3)) along the span. Black line: maximal number of gusts, circles: gusts limited to the enlarged criterion, gray line: super-critical gusts.

If the frequency of the excitation is lower than $f_{c,k}$ then all the cascade modes k are cut-off and the gust is called sub-critical. Otherwise at least one cascade mode is cut-on and the gust is said super-critical. Hanson (2001) defines an interval of k_r in order to consider only the super-critical gusts in the cascade response : $-k_{r,max} < k_r < k_{r,max}$ with $k_{r,max} = qB\Omega/\beta c_0$. However even if the cut-off cascade modes do not directly radiate to the far-field their corresponding $\Delta\hat{P}$ is non zero and may contribute because of the rectilinear to annular transformation, as shown by Posson et al. (2011) in broadband noise studies. Thus an enlarged criterion is defined as $[-k_{r,max} - \Delta k_r, k_{r,max} + \Delta k_r]$ with $\Delta k_r C = 20$. Figure 4 validates this enlarged criterion for the present test case. It compares the cascade response along the span for different frequencies and duct modes computed with

only the super-critical gusts, with only the gusts corresponding to the enlarged criterion and with the maximal number of gusts. It is shown that the proposed criterion allows reproducing the whole response. Moreover Fig. 4 indicates that the sub-critical gusts have more influence at low frequencies, which is consistent with the results of Posson et al. (2011) for the acoustic power in a broadband noise context.

Vane response

The cascade response using the 3D gusts methodology presented here is obtained using Eq. (2), and compared to the unsteady vane loading given by the flow simulation. Figure 5 presents the dimensionless pressure jumps $\Delta\hat{P}_q(x', r)/\rho_0 c_0^2$ along the duct span at midchord, for the considered harmonics. The 2D response coming from de Laborderie et al. (2012) is added to the comparisons. It is shown that the skewed gusts have an important effect on the cascade response, both on the amplitude and on the shape of the acoustic sources. Indeed the amplitude given by the 3D model tends to be closer to the CFD response than the 2D model, thus confirming that a real 3D model yields more realistic acoustic sources. See for instance the lower half part of the response at 2BPF, where the 3D model reproduces the CFD result well. However a limitation to this conclusion concerns the increased number of peaks in the 3D response compared to the 2D model. In future studies the position where the excitation is extracted will be investigated as a location closer to the vanes could reduce the global over-estimation given by the model. A correction of the unsteady vane loadings proposed by Posson et al. (2010) will also be applied as it should reduce their oscillatory behavior. It consists in a modification of the radial wavenumber of the excitation in order to consider some annular effects.

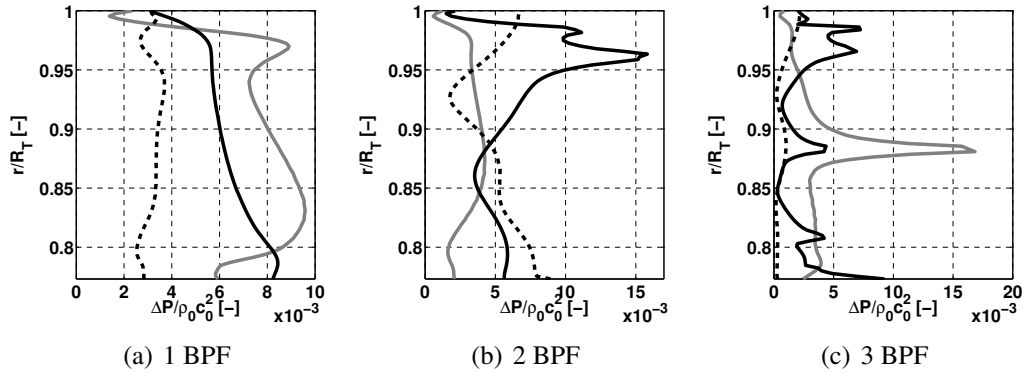


Figure 5: Amplitude of the dimensionless pressure jump at midchord along the span. Gray line: 2D model, black line: 3D model, dash line: CFD.

Discontinuities along the duct span

As explained in the first paragraph of this section a rectilinear cascade radiates acoustic modes governed by their cut-off frequency $f_{c,k}$ (Eq. 5). The latter depends on the geometry of the cascade that varies along the span because the model is based on a strip theory approach. Thus for a given frequency of the excitation a cascade mode may become cut-on at specific radial locations. This particularity of radial strip based models has already been highlighted by Elhadidi et al. (2003). Figure 6(a) presents the cut-off frequencies of some cascade modes k for two different gusts: ($q = 2, |n| = 1$) and

($\bar{q} = 3, |n| = 2$). For the second gust the cut-off frequency plotted is very close to the 3 BPF at two locations. This can create numerical issues in the model that are visible as the peaks located at similar positions in Fig. 5 (c). At 2 BPF Fig. 6(a) indicates a similar behavior near $r/R_T = 1$ possibly responsible for the peak close to the tip in Fig. 5 (b).

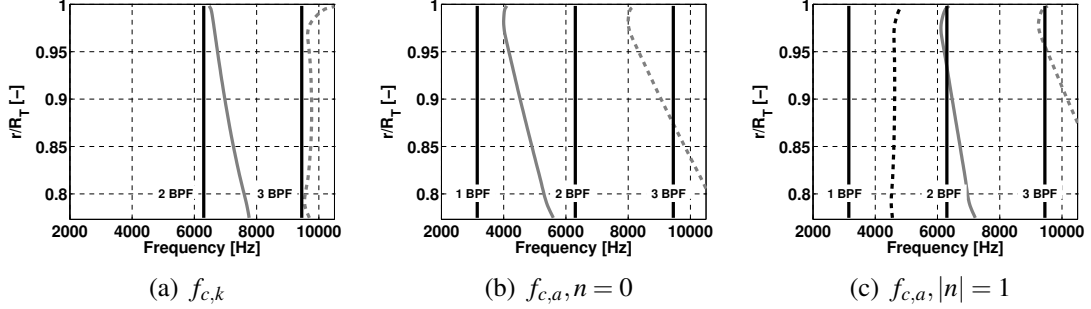


Figure 6: Variation along the span of the cut-off frequencies of the cascade modes (a) and of the passage modes (b)(c). Figure (a): line: gust ($\bar{q} = 2, |n| = 1$), cascade mode $k = 1$; dash line: gust ($\bar{q} = 3, |n| = 2$), cascade mode $k = 3$. Figures (b)(c): black dash line: $a = 0$; gray line: $a = 1$; gray dash line: $a = 2$.

Moreover in each equivalent rectilinear cascade the overlapping part corresponds to waveguides in which inter-vane channel modes may propagate. Glegg (1999) gives the cut-off frequency of such modes of order a depending on the variable solidity along the span:

$$f_{c,a} = \pm \frac{c_0 \beta}{2\pi} \sqrt{\left(\frac{a\pi}{h}\right)^2 + k_r^2}. \quad (6)$$

Thus $f_{c,a}$ is independent of σ and can be plotted along the span for different values of k_r . When $k_r = 0$ (Fig. 6(b)) the passage mode $a = 2$ is cut-off below midspan at 3 BPF and cut-on in the upper part of the span. This behavior explains the peak observed in Fig. 5 (c) around midspan, both for the 3D and 2D models. Indeed in the latter only the gust with $k_r = 0$ appears creating a peak with a larger amplitude than the 3D model. In Fig. 6(c) the passage modes of orders $a = 1$ and $a = 2$ are successively cut-off and cut-on along the radius at 2 and 3 BPF respectively, creating the peaks in Figs. 5 (b) and (c) around $r/R_T = 0.95$.

Finally from this analysis the difference between a 2D and a 3D cascade response is clarified. Indeed more skewed gusts are considered in the latter (only $k_r = 0$ in 2D) thus more cascade modes and inter-vane channel modes are created. Consequently it is likely to obtain more peaks in a 3D response than in a 2D response. However on this test case the discontinuities existing in 2D are damped with the 3D model and it would be interesting to confirm this point with other test cases.

RESULTS - ACOUSTIC POWER

Following the acoustic analogy of Goldstein (1976), the acoustic powers radiated upstream and downstream of the compressor stage are computed. Only the excited and cut-on duct modes radiate acoustic energy, so the results are presented as modal acoustic powers in Fig. 7, with all the radial duct mode powers summed at each corresponding

azimuthal mode. The results given by the 3D model are compared to those of the 2D model and to those obtained by making the unsteady vane loading given by the simulation radiate with the same acoustic analogy, from de Laborderie et al. (2012). These results have to be linked to the cascade response studied in Fig. 5. Indeed at 1 BPF the acoustic source given by the 3D model is closer to the CFD than the 2D model for most of the span. However this is barely the case in Fig. 7 (d) where the 3D model slightly predicts a power closer to the reference than the 2D model, but is further away for the upstream propagation in Fig. 7 (a). At 2 BPF the upstream propagation of the mode 20 is well predicted by the 3D model but the other modes are over-predicted at this frequency. This is probably caused by the large peak brought by the 3D model and discussed above. Finally at 3 BPF the 3D model gives a better prediction than the 2D model for half of the modes. As explained in the previous section the amplitude of the acoustic sources given by the 3D model are closer to the CFD data than the 2D model but more discontinuities are created when considering several skewed gusts. These peaks observed along the span are responsible for the mitigate comparison in terms of acoustic power. Thus it would be interesting to impose a correction to limit these peaks, not present in a real geometry, since away from these discontinuities the 3D model tends to give a realistic response.

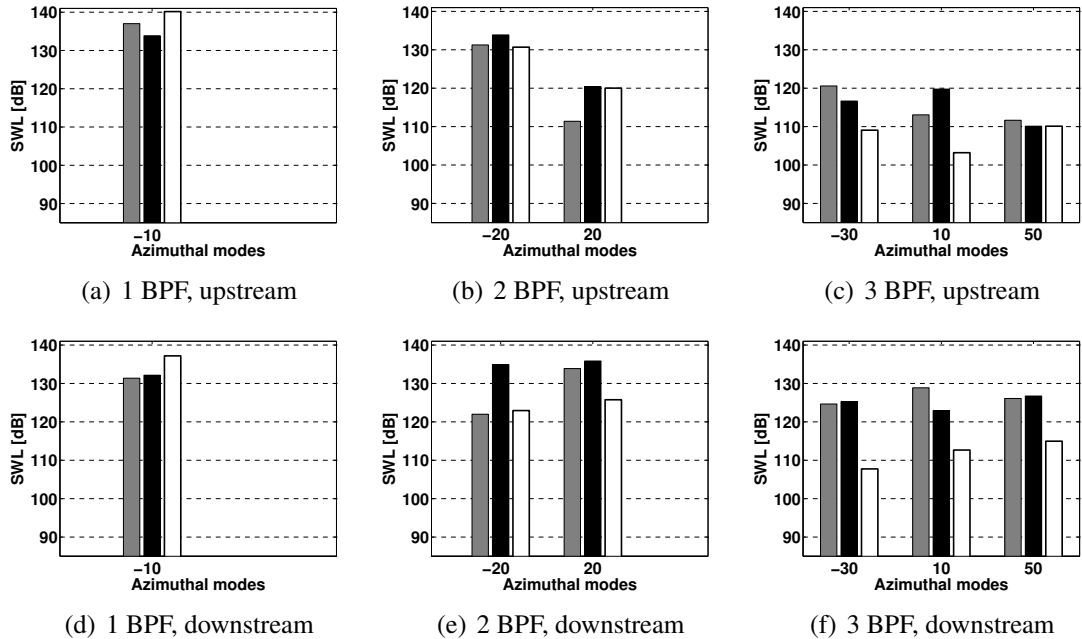


Figure 7: Modal acoustic power radiated upstream and downstream within the annular duct. Gray: 2D model, black: 3D model, white: CFD sources.

CONCLUSION

This work evaluates the effect of considering skewed gusts in a cascade based acoustic model for fan tonal noise prediction. An unsteady flow simulation of an axial compressor stage provides both the vortical excitation and the actual tonal noise sources. The methodology which consists in decomposing the excitation in the radial direction is validated. As expected the 3D cascade response is globally closer to the CFD results than the response of the 2D model since the skewed gusts allow to better account for the span-

wise variation of the incident excitation. However more discontinuities appear in the 3D response along the duct span and their origins that are related to the strip theory approach are explained. They mitigate comparisons in terms of modal acoustic powers where the 3D model provides a better noise prediction than the 2D version in about half of the cases. In future studies an annular geometry correction will be used in the cascade response, thus the acoustic prediction given by this 3D model should be improved.

REFERENCES

- [1] V. Blandeau, T. Node-Langlois, J. de Laborderie, L. Soulat, S. Moreau, and H. Posson. Camber effects in cascade-gust interaction noise through a simple extension of analytical models. In *18th AIAA/CEAS Aeroacoustics Conference*, number AIAA-2012-2307, [2012].
- [2] J. de Laborderie, S. Moreau, A. Berry, and H. Posson. Several technological effects on tonal fan noise prediction. In *18th AIAA/CEAS Aeroacoustics Conference*, number AIAA-2012-2131, [2012].
- [3] B. Elhadidi, H. M. Atassi, and W. K. Blake. Acoustic and hydrodynamic response of an annular cascade to inflow disturbances in swirling flows. In *4th ASME/JSME Joint Fluids Engineering Conference*, [2003].
- [4] S. A. L. Glegg. The response of a swept blade row to a three-dimensional gust. *Journal of Sound and Vibration*, 227(1):29–64, [1999].
- [5] M. E. Goldstein. *Aeroacoustics*. McGraw-Hill, New York, [1976].
- [6] D. B. Hanson. Theory for broadband noise of rotor and stator cascades with inhomogeneous inflow turbulence including effects of lean and sweep. Technical Report NASA-CR-210762, NASA, [2001].
- [7] A. E. D. Lloyd and N. Peake. Rotor-stator broadband noise prediction. In *14th AIAA/CEAS Aeroacoustics Conference*, number AIAA-2008-2840, [2008].
- [8] H. D. Meyer and E. Envia. Aeroacoustic analysis of turbofan noise generation. Technical Report NASA-CR-4715, [1996].
- [9] H. Posson, S. Moreau, and M. Roger. On the use of an uniformly valid analytical cascade response function for fan broadband noise predictions. *Journal of Sound and Vibration*, 329:3721–3743, [2010].
- [10] H. Posson, S. Moreau, and M. Roger. Broadband noise prediction of fan outlet guide vane using a cascade response function. *Journal of Sound and Vibration*, 330:6153–6183, [2011].
- [11] L. Soulat, S. Moreau, and H. Posson. Wake model effects on the prediction of turbulence-interaction broadband noise in a realistic compressor stage. In *41st AIAA Fluid Dynamics Conference and Exhibit*, number AIAA-2011-3900, [2011].
- [12] J. M. Tyler and T. G. Sofrin. Axial flow compressor noise studies. *Society of Automotive Engineers Transactions*, 70:309–332, [1962].